

Mutations in *ZMYND10*, a Gene Essential for Proper Axonemal Assembly of Inner and Outer Dynein Arms in Humans and Flies, Cause Primary Ciliary Dyskinesia

Daniel J. Moore,^{1,17} Alexandros Onoufriadis,^{2,3,17} Amelia Shoemark,⁴ Michael A. Simpson,⁵ Petra I. zur Lage,¹ Sandra C. de Castro,^{3,6} Lucia Bartoloni,⁷ Giuseppe Gallone,¹ Stavroula Petridi,^{2,3} Wesley J. Woollard,⁵ Dinu Antony,^{2,3} Miriam Schmidts,^{2,3} Teresa Didonna,⁷ Periklis Makrythanasis,⁷ Jeremy Bevilard,⁷ Nigel P. Mongan,⁸ Jana Djakow,⁹ Gerard Pals,¹⁰ Jane S. Lucas,¹¹ June K. Marthin,¹² Kim G. Nielsen,¹² Federico Santoni,⁷ Michel Guipponi,^{7,13} Claire Hogg,⁴ Stylianos E. Antonarakis,^{7,13,14} Richard D. Emes,^{8,15} Eddie M.K. Chung,¹⁶ Nicholas D.E. Greene,^{3,6} Jean-Louis Blouin,^{7,13} Andrew P. Jarman,^{1,18,*} and Hannah M. Mitchison^{2,3,18}

Primary ciliary dyskinesia (PCD) is a ciliopathy characterized by airway disease, infertility, and laterality defects, often caused by dual loss of the inner dynein arms (IDAs) and outer dynein arms (ODAs), which power cilia and flagella beating. Using whole-exome and candidate-gene Sanger resequencing in PCD-affected families afflicted with combined IDA and ODA defects, we found that 6/38 (16%) carried biallelic mutations in the conserved zinc-finger gene *BLU* (*ZMYND10*). *ZMYND10* mutations conferred dynein-arm loss seen at the ultrastructural and immunofluorescence level and complete cilia immotility, except in hypomorphic p.Val16Gly (c.47T>G) homozygote individuals, whose cilia retained a stiff and slowed beat. In mice, *Zmynd10* mRNA is restricted to regions containing motile cilia. In a *Drosophila* model of PCD, *Zmynd10* is exclusively expressed in cells with motile cilia: chordotonal sensory neurons and sperm. In these cells, P-element-mediated gene silencing caused IDA and ODA defects, proprioception deficits, and sterility due to immotile sperm. *Drosophila Zmynd10* with an equivalent c.47T>G (p.Val16Gly) missense change rescued mutant male sterility less than the wild-type did. Tagged *Drosophila ZMYND10* is localized primarily to the cytoplasm, and human ZMYND10 interacts with LRRC6, another cytoplasmically localized protein altered in PCD. Using a fly model of PCD, we conclude that ZMYND10 is a cytoplasmic protein required for IDA and ODA assembly and that its variants cause ciliary dysmotility and PCD with laterality defects.

Motile cilia are present on various epithelial surfaces, including the respiratory airways, brain ependyma, and fallopian tubes, and are structurally similar to sperm flagella.¹ Their core axoneme is composed of nine peripheral outer doublet microtubules surrounding a central-pair microtubule apparatus (9+2 arrangement), whereas motile embryonic node monocilia lack the central-pair apparatus (9+0 arrangement). Structures attached along the axoneme govern ciliary beating via a highly regulated and synchronous sliding between microtubules (inner-dynein-arm [IDA] and outer-dynein-arm [ODA] motor complexes) and regulate dynein activity (radial spokes and nexin-dynein regulatory complexes). Studies of ciliated organisms, including *Chlamydomonas*, *Paramecium*,

Xenopus, *Planaria*, trypanosomes, and *Drosophila*,^{2–4} have helped to show that the axoneme is a superstructure facilitating both axoneme bending via the dynein motors' ability to walk along the microtubules in a minus-ended fashion⁵ and signal communication between the central apparatus and dynein arms to regulate ciliary motility.

Primary ciliary dyskinesia (PCD [MIM 244400]) is a genetically heterogeneous autosomal-recessive disorder affecting 1 in 15,000–30,000 births and is caused by abnormal function of motile cilia and flagella.^{6–8} Abnormal motility is associated with axonemal ultrastructural defects, giving rise to symptoms including sinopulmonary disease, which is due to impaired mucociliary transport in the airways and which manifests with

¹Centre for Integrative Physiology, School of Biomedical Sciences, University of Edinburgh, George Square, Edinburgh EH8 9XD, UK; ²Molecular Medicine Unit, Institute of Child Health, University College London, London WC1N 1EH, UK; ³Birth Defects Research Centre, Institute of Child Health, University College London, London WC1N 1EH, UK; ⁴Department of Paediatric Respiratory Medicine, Royal Brompton and Harefield NHS Foundation Trust, London SW3 6NP, UK; ⁵Division of Genetics and Molecular Medicine, King's College London School of Medicine, Guy's Hospital, London SE1 9RT, UK; ⁶Neural Development Unit, Institute of Child Health, University College London, London WC1N 1EH, UK; ⁷Department of Genetic Medicine and Development, University of Geneva School of Medicine, 1211 Geneva 4, Switzerland; ⁸School of Veterinary Medicine and Science, University of Nottingham, Leicestershire LE12 5RD, UK; ⁹Department of Paediatrics, 2nd Faculty of Medicine, Charles University in Prague and Motol University Hospital, 150 06 Prague 5, Czech Republic; ¹⁰Department of Clinical Genetics, VU University Medical Center, PO Box 7057, 1077 MC Amsterdam, the Netherlands; ¹¹Primary Ciliary Dyskinesia Centre, NIHR Respiratory Biomedical Research Unit, University of Southampton and University Hospital Southampton NHS Foundation Trust, Southampton SO16 6YD, UK; ¹²Paediatric Pulmonary Service, Department of Paediatric and Adolescent Medicine, Copenhagen University Hospital, Rigshospitalet, 2100 Copenhagen, Denmark; ¹³Division of Genetic Medicine, University Hospitals of Geneva, 1211 Geneva 4, Switzerland; ¹⁴Institute of Genetics and Genomics, Geneva University Medical Center, University of Geneva, 1211 Geneva 4 Switzerland; ¹⁵Advanced Data Analysis Centre, University of Nottingham, Sutton Bonington Campus, Leicestershire LE12 5RD, UK; ¹⁶General and Adolescent Paediatric Unit, Institute of Child Health, University College London, London WC1E 6DE, UK

¹⁷These authors contributed equally to the work

¹⁸These authors contributed equally to the work

*Correspondence: andrew.jarman@ed.ac.uk

<http://dx.doi.org/10.1016/j.ajhg.2013.07.009>. ©2013 by The American Society of Human Genetics. All rights reserved.

perinatal respiratory distress, chronic respiratory infections, rhinosinusitis, otitis media, and bronchiectasis.⁸ Subfertility can occur in both sexes, and in about half of affected individuals, situs abnormalities are linked to isomerism and, in some cases, congenital heart defects;⁹ hydrocephalus is a rare association. Mutations that cause PCD have been reported in 19 genes, all of which are associated with various ultrastructural defects, in addition to *RPGR* (MIM 312610), mutations in which might contribute to syndromic PCD.¹⁰ These 19 genes include those encoding axonemal proteins of the ODA or its docking complex (DNAH5, DNAH11, DNAI1, DNAI2, DNAL1, TXNDC3, and CCDC114),^{11–18} the radial spoke heads (RSPH4A and RSPH9),¹⁹ the central-pair apparatus (HYDIN),²⁰ or the nexin-dynein regulatory complexes (CCDC164, CCDC39, and CCDC40).^{21–23}

A distinct set of six proteins altered in PCD are either solely localized to the cytoplasm or found in both the cytoplasm and the axoneme: DNAAF1 (LRRC50), DNAAF2 (KTU), DNAAF3, CCDC103, HEATR2, and LRRC6.^{24–30} These are most likely involved in the cytoplasmic preassembly of dynein-arm complexes prior to their movement into the axoneme and/or in axonemal transport and attachment processes for the dynein-arm complexes. Variants in these six proteins are associated with a simultaneous ODA and IDA loss, a defect found in a significant proportion (24%–45%) of PCD cases (the variability is due in part to the difficulty in visualizing the IDA by transmission electron microscopy [TEM]).^{31–33} To determine the full spectrum of genetic defects causing IDA and ODA loss in individuals affected by PCD, we analyzed 38 unrelated PCD-affected families, representing a total of 60 affected individuals displaying reduced or absent IDA and ODAs in nasal biopsies. Signed and informed consent was obtained from all participants according to protocols approved by the institutional ethics review boards, and all cases were diagnosed with classic clinical PCD symptoms, including recurrent respiratory tract infections, chronic sinusitis, rhinitis, otitis media, bronchiectasis, and laterality and fertility defects.

We first used next-generation whole-exome sequencing (WES) to analyze an affected individual from 11 of these PCD-affected families by performing exome capture by in-solution hybridization followed by massively parallel sequencing. Approximately 3 µg of genomic DNA was sheared to a mean fragment size of 150 bp (Covaris), and the fragments were used for Illumina paired-end DNA library preparation and enrichment for target sequences (Agilent). Enriched DNA fragments were sequenced with 100 bp paired-end reads (HiSeq2000 platform, Illumina). Sequencing reads were aligned to the reference human genome with Novoalign (Novocraft Technologies) and the Burrows-Wheeler Aligner. Duplicate and multiple mapping reads were excluded, and the depth and breadth of sequence coverage was calculated with the use of custom scripts and the BedTools package.³⁴ Single-nucleotide substitutions and small indels were identified with SAMtools

and Pindel and were annotated with the ANNOVAR tool. Variant calling was performed with a previously published in-house pipeline.³⁵ More than 5 Gb of sequence was generated per sample; >75% of the target exome was present at >20-fold coverage, and >95% was present at 5-fold coverage. We focused on homozygous and compound-heterozygous nonsynonymous or splice-site substitutions or indels that are either absent from or present with a frequency < 0.01 in the 1000 Genomes Project.³⁶ We further filtered variants by removing any that are present at a frequency > 0.01 in 700 in-house non-PCD control exomes.

We found that out of a total of 23, 21, and 24 biallelic variants of interest fitting the filtering criteria, biallelic variants in *ZMYND10* (MIM 607070; RefSeq accession number NM_015896.2) were shared by one affected individual from each of families UCL-88, UCL-142, and UCL-157, respectively. *ZMYND10* is present in the Cildb ciliome database.³⁷ It was also reported to have a likely role in ciliary motility because its expression is 14-fold higher in ciliated primary human airway epithelial cells upon stimulation of ciliogenesis by transfer to air-liquid interface culture³⁸ and from expression profiling of bronchial biopsies from PCD cases.³⁹ The exome-sequencing coverage in the three affected individuals is detailed in Table S1, available online, and their variant calling and filtering are summarized in Tables S2 and S3. All three cases are of North European descent, and two (UCL-142 II:1 from a genetic isolate and UCL-157 II:5 from a first-cousin consanguineous union) are homozygous for a *ZMYND10* c.47T>G (p.Val16Gly) missense substitution, whereas the other (UCL-88 II:2) is compound-heterozygous for c.47T>G (p.Val16Gly) and a frameshift deletion (c.589_590del). The National Heart, Lung, and Blood Institute (NHLBI) Exome Sequencing Project Exome Variant Server reveals six carriers of c.47T>G (p.Val16Gly) in 4,300 European control exomes, corresponding to a low frequency of 0.000698 (rs138815960); this variant is absent from all 700 in-house control exomes.

Segregation analysis of the identified variants by Sanger sequencing in other available members of the three families confirmed the recessive inheritance of both variants (Figure 1A and Figure S1). Three more unrelated PCD cases carrying *ZMYND10* variants were then identified from Sanger sequencing of *ZMYND10* in a cohort of 27 additional individuals with ODA and IDA defects: North European origin individuals GVA-09 II:2 and UCL-233 II:1 are, respectively, homozygous for a missense variant (c.797T>C [p.Leu266Pro]) and compound-heterozygous for two missense substitutions (c.47T>G [p.Val16Gly] and c.116T>C [p.Leu39Pro]), whereas UCL-226 from a UK-Pakistani family arising from a first-cousin marriage is homozygous for a frameshift deletion (c.65delT [p.Phe22Serfs*21]) (Figure 1A). The mutations in family GVA-09, first described in 2000 as showing linkage to *ZMYND10* with a “potentially interesting” maximum nonparametric LOD score of 1.41,⁴⁰ were also detected

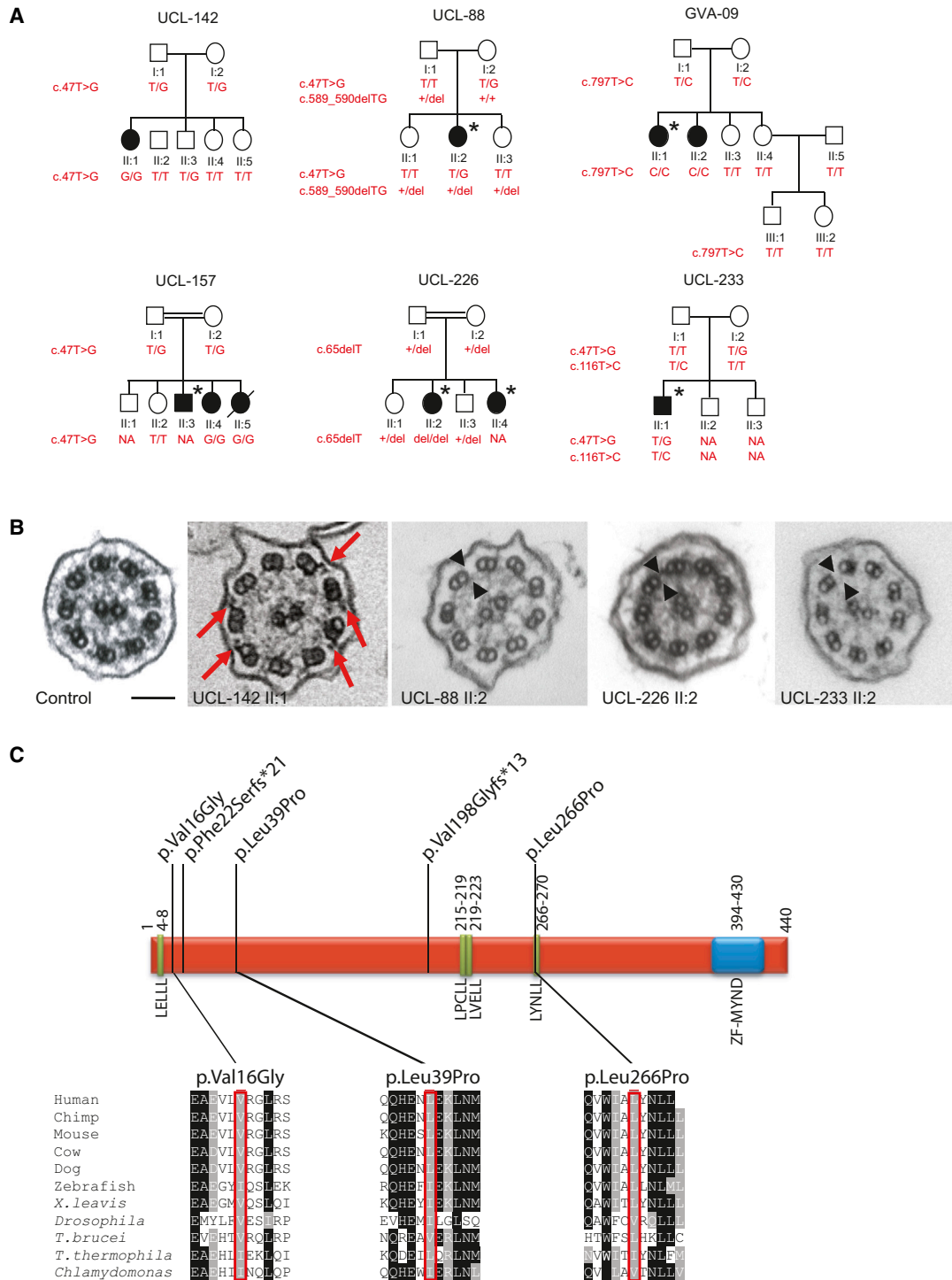


Figure 1. Family Segregation Analysis, Cilia Ultrastructure, and Localization of Variants within the Predicted ZMYND10

(A) Pedigree structure and segregation analysis of the six PCD-affected families harboring *ZMYND10* mutations. Filled symbols indicate affected individuals, an asterisk indicates the laterality defect, and a slash indicates that an individual is deceased. Plus signs indicate a normal allele, and “NA” indicates that the result is not available.

(B) TEM shows that the nasal respiratory epithelial cell cilia of *ZMYND10*-mutant cases have either fewer (red arrows indicate remnant arms) or no (black arrowheads) IDAs and ODAs in comparison to those of the control. Scale bar represents 100 nm.

(C) Location of *ZMYND10* variants. Green boxes indicate LxxLL motifs, the blue box represents the ZF-MYND domain, and the amino acid positions are shown. Conservation across species of residues affected by the three missense variants is shown with proteins (corresponding accession numbers are shown in parentheses) from the following species: *H. sapiens* (RefSeq NP_056980.2), *P. troglodytes* (RefSeq XP_516479.2), *M. musculus* (RefSeq NP_444483.2), *B. taurus* (RefSeq NP_001035638.1), *C. lupus* (RefSeq XP_533818.1), *D. rerio* (RefSeq NP_956691.1), *X. leavis* (RefSeq NP_001090272.2), *D. melanogaster* (RefSeq NP_648625.1), *T. brucei* (RefSeq XP_828897.1), *T. thermophila* (RefSeq XP_001026696.1), and *C. reinhardtii* (Phytozome accession Cre08.g358750.t1.3). The transcript annotations are based on the Augustus update u11.6 annotation of Joint Genome Institute assembly v.5.

in a separate WES study performed on the two affected children and their unaffected sibling, II:3 (Table S4). Here, after filtering, *ZMYND10* was the best scored option with reference to autosomal-recessive inheritance of variant homozygosity in this consanguineous pedigree (Table S5). Segregation analysis was performed in all three families and was again consistent with an autosomal-recessive disease-inheritance pattern (Figure 1A and Figure S1).

The mutation summary and clinical information for the affected individuals carrying *ZMYND10* mutations from all six families are shown in Table S6. The missense substitutions (p.Val16Gly, p.Leu39Pro, and p.Leu266Pro) were predicted to be “damaging” and “probably damaging” by SIFT and PolyPhen-2, respectively. Moreover, all three residues affected by missense variants are well conserved in *ZMYND10* orthologs in other ciliated species (Figure 1C and Figure S2). Protein modeling shows that *ZMYND10* contains four conserved classical LxxLL protein-binding motifs, in addition to its C-terminal MYND zinc-finger domain, implying that it requires interacting partners for its function. In proteins of this family, amino acid substitutions at any of the leucines within the LxxLL motif abrogate function.⁴¹ The first residue of the *ZMYND10* LYNLL motif (at residues 266–270), which is the best conserved motif across vertebrates and also in the flagellate protozoan *Trypanosoma brucei*, is changed by the p.Leu266Pro missense variant in family GVA-09. This proline substitution might be damaging by creating a kink in the predicted coiled LxxLL motif, and this lends support to the functional significance of this motif (Figure 1C).

TEM of nasal biopsy respiratory cilia cross-sections (prepared as previously reported³²) from individuals UCL-142 II:1, UCL-88 II:2, UCL-226 II:2, and UCL-233 II:2 detected in all cases a loss of IDAs and ODAs at the ultrastructural level (Figure 1B). In individual UCL-142 II:1 (with homozygous p.Val16Gly), we noticed an apparently intermediate phenotype in nasal respiratory cilia and variable retention of the IDAs and ODAs in different cross-sections. The absence of IDAs and ODAs in cilia axonemes was further confirmed in UCL-88 II:2 by high-resolution immunofluorescence staining for the ODA component DNAH5 and the IDA component DNALI1, respectively, which are now well-established diagnostic markers for PCD dynein-arm defects (Figure S3). An apparent accumulation of staining in the peribasal area of the affected individual’s cilia was noted, especially for DNAH5, indicating that these dynein-arm components might be retained in the cytoplasm, but not successfully assembled and/or transported to the axoneme.

To gain insights into the pathogenic nature of these *ZMYND10* mutations, we performed high-speed video microscopic analysis of the affected individuals’ nasal cilia. Compared to controls, cases showing a complete absence of IDAs and ODAs (UCL-88 II:2, UCL-226 II:2, and UCL-233 II:2) had cilia that were almost completely static,

consistent with other mutations associated with IDA and ODA defects (Movies S1 and S2).^{24–30} In contrast, a significant motility was retained by cilia from the c.47T>G (p.Val16Gly) homozygous individual UCL-142 II:1 in whom the dynein arms were partially retained. However, there was a slowed and stiff beating pattern that lacked the normal beat amplitude (a fully extended forward power stroke and backward recovery stroke) seen in controls (Movies S3 and S4); the reduced ciliary beat frequency had a median of 3.97 Hz (range = 2.92–5.24 Hz) compared to the normal range of 4–7 Hz at room temperature. Consistent with this, the IDAs and ODAs were also reported to be reduced, but not absent, in cilia in affected individuals from family UCL-157, which also carries homozygous c.47T>G (p.Val16Gly) mutations. In addition, cilia motility was recorded as variable in family UCL-157: cilia from affected individual II:4 were almost static, whereas II:5 had more normal motility (Table S6).

ZMYND10 orthologs are found widely in ciliated eukaryotes, and notably, no ortholog exists in *Caenorhabditis elegans*, which has only immotile cilia. There is, however, an ortholog in both *Ostreococcus*, a green alga that lacks cilia but retains IDA genes, and *Physcomitrella*, a moss with motile flagellated sperm. The mouse ortholog (*Zmynd10*) is enriched in the testes and is 1 of 99 genes whose expression pattern is correlated with tissues rich in ciliated cells.⁴² In humans, alternative splicing leads to two *ZMYND10* isoforms differing across 35 centrally positioned amino acids; these are expressed in the testes and lungs (we note that the five sequence variants identified here would equally affect both transcripts).⁴³ *ZMYND10* (also known as *BLU*) is within a tumor-suppressor gene cluster in chromosomal region 3p21.3 and has been found to be inactivated in common human cancers, including lung, nasopharyngeal, and ovarian cancers, but no susceptibility variants have been identified as of yet.⁴⁴

To investigate the ciliary role of *ZMYND10*, we determined the tissue distribution of *Zmynd10* expression in mouse embryos at embryonic day 18.5 by in situ hybridization as previously described.¹⁹ This showed specific expression in the ciliated epithelial layer associated with nasal and lung epithelium (Figures 2A and 2B and Figure S4). This restricted expression in regions where motile cilia are located replicates the localization pattern of other proteins that cause PCD when deficient.^{11,19} For functional evaluation of *ZMYND10*, we turned to a *Drosophila* model using flies maintained on standard media at 25°C and a *w¹¹¹⁸* strain as a wild-type control. In *Drosophila*, sensory neurons and sperm are the only cells that bear cilia or flagella. We recently noted that the *Drosophila* ortholog of *ZMYND10*, *CG11253* (referred to here as *Zmynd10*), is highly expressed in the transcriptome of developing chordotonal (Ch) sensory neurons,⁴⁵ which are proprioceptors with motile mechanosensory cilia.⁴⁶ In situ hybridization of whole embryos by standard methods with the use of a digoxigenin-labeled RNA probe³ confirmed that during embryogenesis *Zmynd10* mRNA

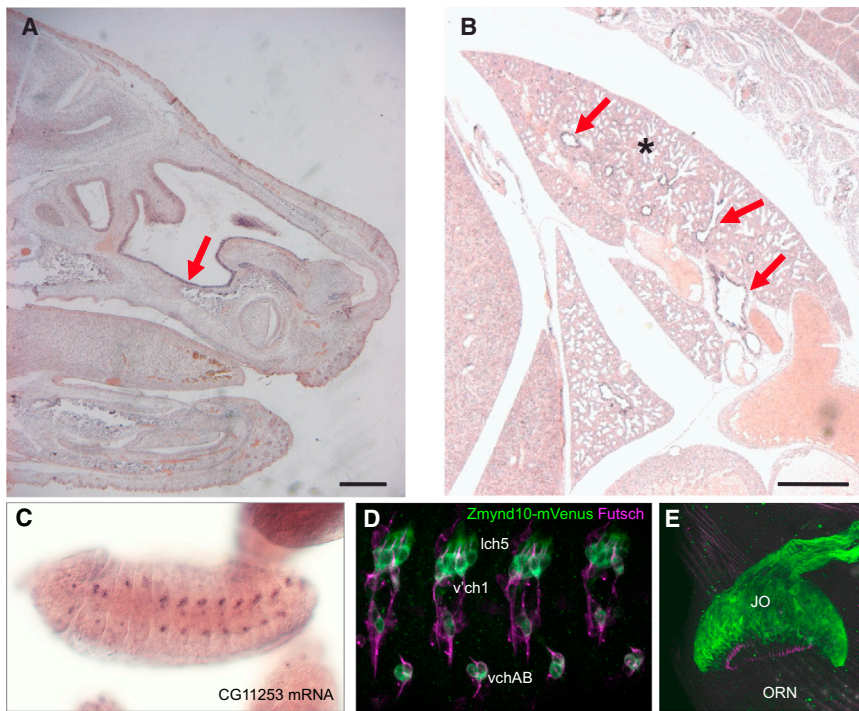


Figure 2. Restricted Expression of ZMYND10 within Motile Ciliated Tissues

(A and B) Expression of *Zmynd10* mRNA in embryonic day 18.5 mouse embryos by whole-mount in situ hybridization reveals specific expression in the nasal epithelium (A, arrow) and the bronchi (B, arrows) of the lung (indicated by an asterisk). Scale bars represent 0.5 mm.

(C) Expression of *Zmynd10* (CG11253) in *Drosophila* embryos by whole-mount in situ hybridization reveals expression restricted to differentiating Ch neurons.

(D) The *Drosophila* *Zmynd10-mVenus* fusion gene (green) is expressed in Ch neurons (lch5, vch5, and vchAB), but not other ciliated sensory neurons (marked by FUTSCH, magenta) in the embryo.

(E) In the pupal antenna, the *Zmynd10-mVenus* fusion gene is strongly expressed in the Ch neurons of Johnston's Organ ("JO"), but not the olfactory receptor neurons ("ORN").

was restricted to developing Ch neurons and was notably absent from other ciliated sensory neurons (Figure 2C and Figures S5A–S5D). This is mirrored by the expression of a *Zmynd10-mVenus* fusion gene, which was constructed from the entire *Zmynd10*, including 1.5 kb of upstream flanking sequence (Figure S5I). The *Zmynd10-mVenus* fusion gene was expressed in embryonic Ch neurons (Figure 2D). In the pupal antenna, the fusion gene was also expressed exclusively in the Ch neurons of Johnston's organ; these cells are auditory receptors (Figure 2E). Unlike other *Drosophila* sensory cilia, Ch neuron cilia have the hallmarks of motility: the proximal portion of their 9+0 axoneme bears dynein arms (Figure 3H), and Ch ciliary movement is important for auditory transduction.^{48,49} Moreover, genetic perturbation of dynein-arm components causes *Drosophila* to be deaf⁵⁰ and also perturbs proprioception.³ In adults, *Zmynd10* is specifically expressed in the testes.⁵¹ Thus, *Zmynd10* expression correlates exclusively with the development of cells with flagella or motile cilia.

Transcriptional regulation of *Zmynd10* supports a role in ciliary motility. The transcription factors Fd3F and Rfx were recently shown to coregulate genes for ciliary motility in Ch neurons (including axonemal dynein genes).³ Indeed, Fd3F is related to vertebrate Foxj1, which is strongly linked to the differentiation of cells bearing motile cilia.^{52–54} *Zmynd10* expression in Ch neurons was greatly reduced in *Rfx*⁴⁹ and *fd3F*¹ mutant embryos^{3,55} (Figures S5E–S5G). The region immediately upstream of *Zmynd10* (which supported Ch-neuron-specific expression of the *Zmynd10-mVenus* fusion gene) contains conserved binding motifs for these factors (Figure S5I). In summary, expression of *Zmynd10* is confined to the only *Drosophila* cells bearing a motile cilium or flagellum, and its expres-

sion is dependent on the transcription factors that regulate motile cilia.

Fly stock *p{EPgy2}CG11253^{EY10886}* (obtained from the Bloomington Stock Center [Indiana University]) contains a P element inserted in the last intron of *Zmynd10* (Figure S5I). In situ hybridization showed that *Zmynd10* mRNA appeared to be strongly reduced or absent in embryos homozygous for this P element insertion, indicating a strong loss-of-function mutation (Figure S5H). Homozygous *Zmynd10^{EY10886}* flies are viable and have no visible morphological defects. However, a climbing assay revealed that they are uncoordinated (Figure 3A). This phenotype was not observed in revertant flies in which the P element had been excised from the *Zmynd10* locus, and coordinated locomotion was completely restored by the introduction of the *Zmynd10-mVenus* fusion gene (Figure 3A). Together with expression-pattern data, this suggests that *Zmynd10^{EY10886}* homozygotes have defective proprioception as a result of malfunctioning Ch neurons. Indeed, antennal Ch neurons are also defective, given that *Zmynd10*-mutant flies have recently been reported to be deaf.⁵⁰

Ch neuron structure was examined by immunofluorescence in embryos, larvae, and pupal antennae. No gross morphological defects in Ch neurons or their terminal cilia were observed with morphology markers (Figures 3B–3D). Compartmentalization of the Ch neuron cilium also appeared normal in that it had correctly localized markers of the proximal motile zone (GT335, anti-polyglutamylated tubulin) and distal sensory zone (the TRPN channel, NOMPC)⁵⁶ (Figure S6 and data not shown). This suggests that there are no general defects in ciliogenesis, compartmentalization of the cilium, or intraflagellar

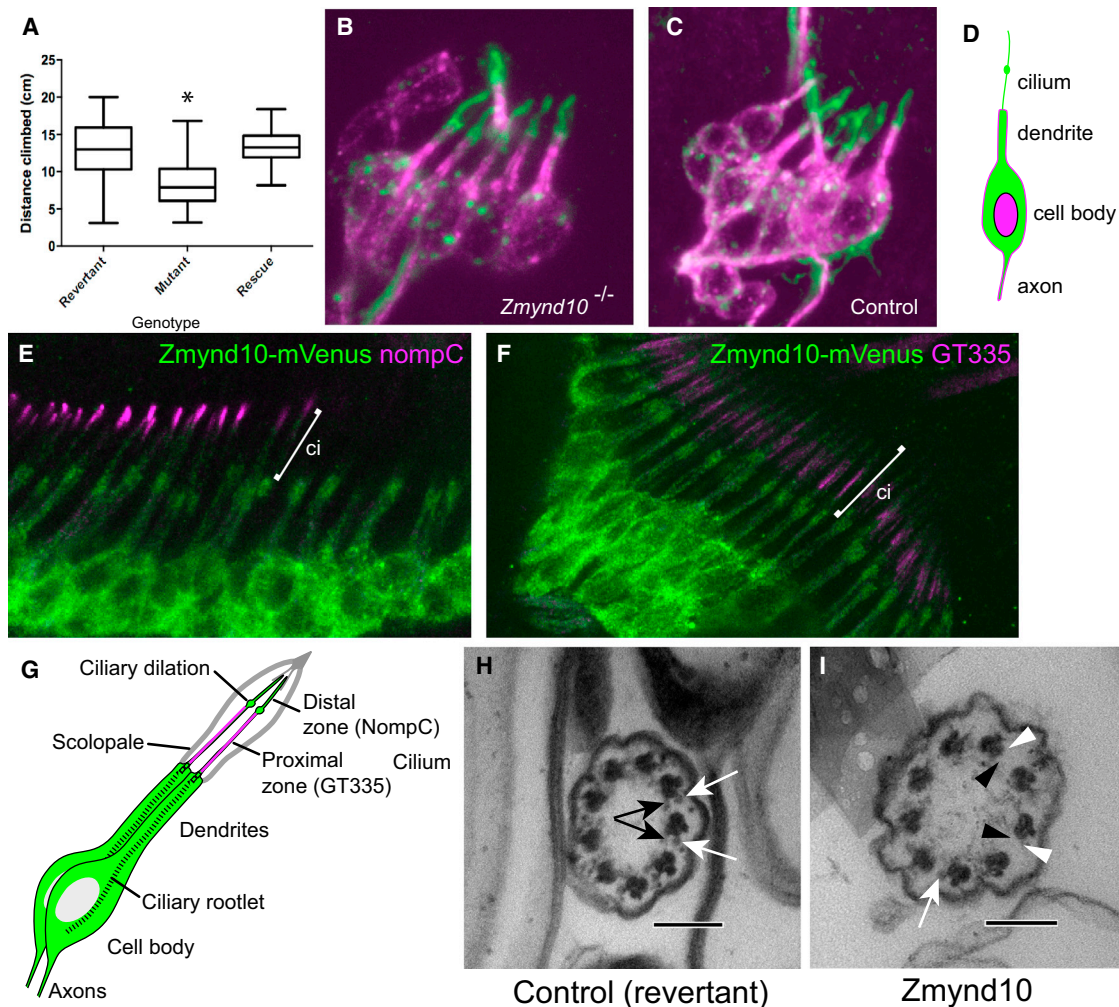


Figure 3. *Zmynd10*-Mutant Flies Have Sensory Defects and Loss of the Axonemal Dynein Arms

(A) A box and whisker plot of climbing assay for proprioceptive defects. Twenty 2- to 7-day-old flies were placed in a measuring cylinder, and then after a 1 min recovery period, they were banged to the bottom of the cylinder, and the height climbed in 10 s was then recorded. Homozygous mutant *Zmynd10*^{EY10886} flies performed significantly less well in this assay than did the “wild-type” revertants (in which the P element had been lost by excision) ($p < 0.0001$). The *Zmynd10-mVenus* fusion transgene completely restored the climbing behavior of homozygous mutant flies (“rescue”). Significance was determined by a Kruskal-Wallis test ($H = 35.48$; $n = 44, 42, \text{ and } 28$; $p < 0.0001$) followed by a Dunn’s test.

(B and C) The Ich5 neuron cluster from an embryonic abdominal segment stained with FUTSCH (magenta) and anti-HRP, which detects the cilium at this stage (green). In mutant embryos, the cilia are present and appear grossly normal in length.

(D) Schematic of embryonic Ch neuron.

(E and F) In Ch neurons in pupal antennae, *Zmynd10-mVenus* expression (green) is largely cytoplasmic relative to *nompC* and *GT335* (distal and proximal ciliary markers, magenta).

(G) Schematic of pupal Ch neurons.

(H and I) TEM of adult antennal Ch neuron cilia. A control with ODA and IDA complexes (white and black arrows, respectively) is indicated in (H). A *Zmynd10* mutant, showing loss of some ODA and IDA complexes (white and black arrowheads, respectively) is shown in (I). Primary antibodies used were mAb-22C10 (1:200), RbAb-HRP (1:500), RbAb-GFP (1:500) (Molecular Probes), mAb-NompC (1:100),⁴⁷ and *GT335* (Sigma, 1:200). Secondary antibodies were from Molecular Probes. Scale bars represent 100 nm.

transport (IFT). Ch cilium ultrastructure was examined by TEM of Johnston’s organ in the adult antenna by Electron Microscopy Research Services, Newcastle University Medical School, as described previously.³ This revealed the presence of a normal 9+0 cilium on each Ch neuron dendrite. However, the proximal axonemal zone showed a reduction in observable dynein arms (Figures 3H and 3I). Both ODAs and IDAs were reduced, and IDAs were possibly affected more strongly (Table S7). Localization of the protein

encoded by *Zmynd10-mVenus* was most strongly observed in the Ch neuron cell bodies, but less reached the inner dendritic segment (Figures 3E–3G). A low level was also observed in the cilium, although this did not extend to the tip.

Homozygous *Zmynd10*-mutant males were infertile given that they produced no offspring when crossed to wild-type females ($n = 60$). In mutant males, the testes appeared normal and contained developing sperm bundles

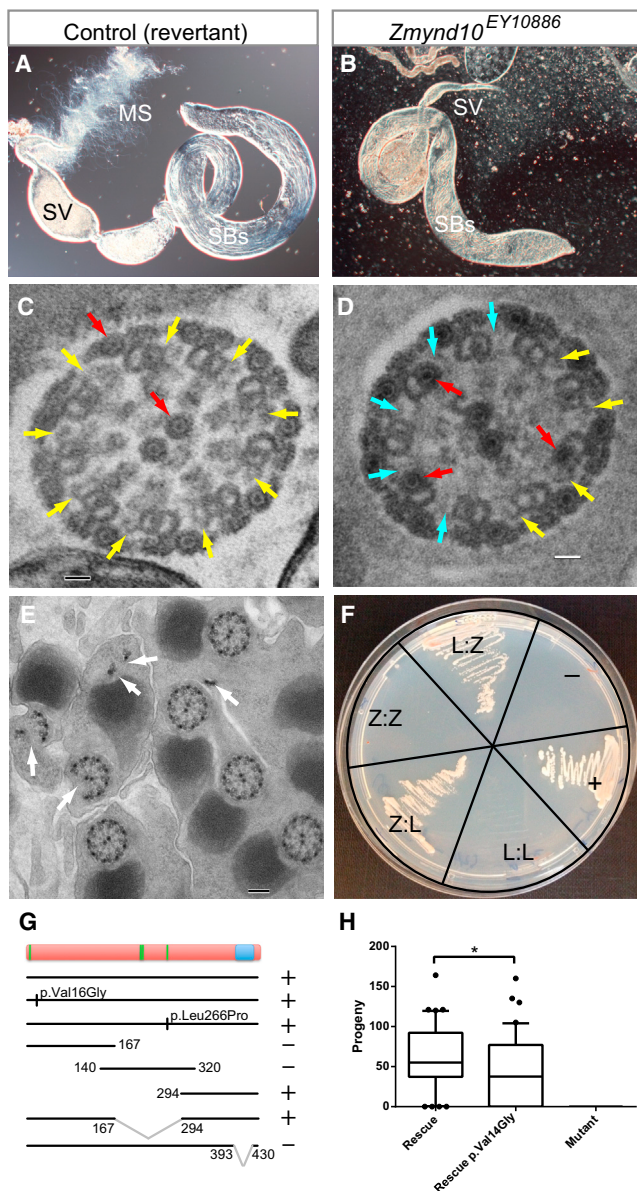


Figure 4. *Zmynd10*-Mutant Male Flies Lack Motile Sperm

(A) In a dissected wild-type adult (5-day-old) testis, sperm bundles (“SBs”) can be seen, the mature sperm are transferred to the seminal vesicle (“SV”), and motile sperm (“MS”) can be seen emerging from this structure.

(B) In a *Zmynd10*-mutant fly, sperm bundles are still observed in the testis, but the seminal vesicle is empty and no motile sperm are seen emerging. There is also some disruption of sperm-bundle coiling at the proximal end of the testis, which might be a secondary effect of sperm immotility.

(C–E) TEM transverse sections of sperm bundles in a testis.

(C) In a control fly, yellow arrows point to dynein arms. Also visible (red arrows) are the inner pair and outer accessory microtubules, which have an electron-dense core (the luminal filament). Scale bar represents 20 nm.

(D) In the mutant, there is loss of dynein arms (cyan arrows) and ectopic luminal filaments in the A microtubule of the doublets (red arrows). Scale bar represents 20 nm.

(E) In the mutant, some flagella have fragmented axonemes (arrows). Scale bar represents 100 nm.

(F) Yeast two-hybrid assay of human ZMYND10 (“Z”) and LRRC6 (“L”). In each sector, the Bait:Prey combinations are indicated. Also present are positive (p53) and negative (Lamin) controls.

(Figures 4A and 4B). TEM showed that the sperm bundles generally consisted of 64 sperm (data not shown), suggesting that spermatocyte divisions and sperm differentiation were largely unaffected. However, motile sperm were never observed in testis dissections; indeed, the seminal vesicles were completely devoid of sperm, suggesting that the sperm were not transferred from the testes to the seminal vesicles (Figures 4A and 4B). This phenotype is similar to that of mutants of *Dic61B*, a testis-specific dynein intermediate chain homolog.⁵⁷

TEM showed sperm flagella with a partial loss of dynein arms (Figures 4C and 4D), and 12% (n = 384) showed axoneme splitting, whereby one or more doublet complexes became detached from the rest of the axoneme (Figure 4E). This might suggest impaired nexin or radial-spoke connections. An additional phenotype was the presence of ectopic luminal filaments (electron-dense cores) within the “A” microtubule of some doublets (Figure 4D). Interestingly, these phenotypes have also been reported to be associated with mutations in the axonemal β 2-tubulin gene *B2t⁶*. Like *Zmynd10*-mutant males, *B2t⁶*-mutant males generate largely intact but immotile sperm with missing ODAs.⁵⁸

Recently, mutations linked to PCD were reported in *LRRC6* (MIM 614930), whose *Drosophila* ortholog is *touch-insensitive larval B (tilB)*.^{29,30} The *tilB*-mutant phenotype, developmental expression pattern, and protein subcellular localization all closely resemble that of mutant *Zmynd10*.^{59,60} These similarities suggest that their two encoded proteins might function together, and indeed, a *Zmynd10* interaction was reported in a large-scale interaction mapping of the *Drosophila* proteome.⁶¹ Given these links, we investigated whether human ZMYND10 and LRRC6 interact. Human ZMYND10 and LRRC6 cDNAs were cloned into pGADT7 activation-domain and pGBKT7 DNA-binding-domain vectors for use in a Matchmaker yeast two-hybrid assay according to the manufacturer’s protocols (Clontech). A clear interaction between these proteins was revealed (Figure 4F). In the same assay, the p.Val16Gly and p.Leu266Pro variants of ZMYND10 still showed interaction with LRRC6 (Figure 4G). Furthermore, deletion analysis of ZMYND10 showed that the

(G) A summary of yeast two-hybrid results of the interaction between LRRC6 and mutated or truncated forms of ZMYND10 shows that interaction (+) is not affected by the PCD-linked protein variants but relies on the presence of the MYND domain. Variants were introduced by site-directed mutagenesis with the use of the Strataclone Quickchange 2 kit (Stratagene).

(H) A box and whisker blot shows the progeny produced by single male flies. *Zmynd10*-mutant males (“mutant”) were infertile, but fertility was restored with the rescue transgene (“rescue”). A two-tailed Mann-Whitney test shows that restoration of fertility was significantly less with a rescue transgene containing the p.Val14Gly missense variant (“rescue V14G”) (U = 586; n = 40, 40; p = 0.0385). For fertility analysis, 40 2- to 5-day-old males were crossed individually to wild-type females. After 2 days of pre-mating, flies were transferred to new vials and were allowed to lay eggs for 3 days. Progeny from the latter were counted.

interaction strictly required the MYND zinc-finger domain (Figure 4G). To further confirm the interaction between the two proteins, we performed a GST pull-down assay on Myc-tagged in-vitro-translated LRRC6 by using either GST or GST-ZMYND10. After electrophoresis of the washed GST samples alongside a sample of the Myc-tagged LRR6 (input), the immunoblot was probed with Myc antibody and showed specific binding of the GST-ZMYND10 only (Figure S7).

We used the fly to model the putative hypomorphic effects of the p.Val16Gly missense variant that correlated with retained ciliary beating activity in affected individuals. We found that fertility and sperm motility in mutant male flies were completely rescued by the introduction of the wild-type *Zmynd10-mVenus* fusion gene. When the PCD-associated variant, p.Val16Gly, was engineered into the fusion gene (p.Val14Gly in the *Drosophila* protein) by site-directed mutagenesis with the StrataClone QuikChange 2 kit (Stratagene), fertility was restored, but not as fully as for the wild-type protein (Figure 4H).

In this study, we have shown that recessive loss-of-function mutations in *ZMYND10* underlie PCD with abnormal axonemal ODA and IDA assembly. This study expands our current understanding of the genetic heterogeneity underlying PCD, given that *ZMYND10* is the seventh gene associated with disease arising from dual IDA and ODA defects and static cilia; in this study, its mutations caused 16% (6/38) of the cases of IDA and ODA defects. We identified two predicted frameshift and three missense variants in *ZMYND10*; notably, one missense change (p.Leu266Pro) affects the first leucine residue of one of the protein's key predicted protein-interaction domains, a conserved LxxLL sequence motif. Being found present on six disease chromosomes in four out of six families affected by *ZMYND10*-associated PCD in this study, the c.47T>G (p.Val16Gly) missense variant could possibly represent a common European-founder-effect mutation, and we investigated this further by deriving haplotype data from SNPs surrounding the variant in the three affected individuals who carry the variant and for whom exome data are available (Table S1). A shared 1.6 Mb haplotype spanning the c.47T>G (p.Val16Gly) variant could be derived, which seems likely to indicate a common ancestral mutation event, but the uninformative nature of the SNP markers within this region prevented firm conclusions (Table S8). These findings can inform future developments in both genetic testing and gene-based therapeutic strategies for PCD and will thus be useful for improved diagnosis, counseling, and carrier testing in families affected by PCD.

In affected individuals, we noted a difference in the ciliary dysmotility conferred between different *ZMYND10* mutations, given that the homozygous inheritance of the c.47T>G (p.Val16Gly) missense variant was found to correlate with retention of cilia motility. The equivalent p.Val16Gly-containing protein was still able to rescue the male infertility phenotype of mutant flies but did so less

completely than the wild-type protein, supporting the idea of some retention of function. Despite the fact that we found a cellular genotype-phenotype correlation for PCD, suggesting that c.47T>G (p.Val16Gly) is a functionally more "mild" allele than a complete null, the clinical significance is unclear: affected individuals carrying the homozygous c.47T>G (p.Val16Gly) mutation still exhibit ineffective mucociliary clearance and classic disease symptoms.

The presence of the LxxLL motifs in the conserved ZMYND10 is intriguing. This motif was first identified in diverse transcriptional coactivators recruited to nuclear receptors in the presence of an agonist, including histone acetyltransferases and histone lysine demethylases (p160s, p300 [also known as CBP], and KDM1A).⁶² Several proteins with LxxLL motifs have been well studied structurally and functionally. Our PCD-associated p.Leu266Pro variant is of interest because it represents an amino acid substitution associated with a human disease in an LxxLL motif. Potentially, ZMYND10 could interact with transcription factors and related coregulator complexes in the cytoplasm and thereby influence the expression of other proteins that are known to cause PCD when deficient. Consistent with this, ZMYND10 has been shown to interact with the TSC22D4 (also known as THG1) corepressor and RNA-processing enzyme.⁶³⁻⁶⁵ However, there is no evidence supporting a direct transcriptional regulatory role for ZMYND10 as of yet. The alternative possibility based on our findings, including the protein interaction revealed between ZMYND10 and LRRC6, is that ZMYND10 plays a direct role in the assembly of the IDAs and ODAs into the axoneme by interacting with the essential family of cytoplasmic dynein-arm preassembly factors that have already been associated with the etiology of PCD. In this case, our study might have identified a mechanism whereby the LxxLL motifs common in transcriptional regulatory complexes play a role in the formation of non-transcription-related complexes, as has been observed for the highly specialized LD motif (LDxLL) found in the paxillin superfamily.⁶⁶ Further studies are therefore warranted to provide insight into the role of the LxxLL motifs identified in ZMYND10 and their potential role in dynein-arm assembly.

We have shown here that *Drosophila* can be used as a suitable model organism for PCD in that it possesses two unique systems available for motile axonemal and cilio-genesis characterization and genetic manipulation: the Ch sensory neurons and the male reproductive system. The heritable mutations mimicking human PCD can be investigated in flies with the use of relatively simple neurological and fertility assays, providing an in vivo platform for modeling PCD-related gene function both for understanding the underlying cellular basis and for testing the ability of PCD-associated variants to rescue the fly mutations. This model will thus be widely applicable to advancing our understanding of the genetic and cellular basis of PCD.

Using this model organism, we determined that *Zmynd10* has a highly restricted expression pattern and function confined to motile-ciliated cells and sperm. The developmental expression of *Zmynd10* in relation to cilium formation in Ch neurons showed that *Zmynd10* expression in developing neurons precedes expression of dynein genes and completion of neuronal terminal differentiation and cilium outgrowth by at least several hours (Figures S5A–S5C),³ which suggests that *Zmynd10* plays a developmental role in dynein-arm synthesis, assembly, or transport. In flies, we were also able to localize ZMYND10 primarily as a cytoplasmic component of cells containing motile cilia. Its mainly cytoplasmic localization is reminiscent of that of three other proteins linked to ODA and IDA loss in PCD: DNAAF1, DNAAF2, and DNAAF3, which are regarded as dynein-arm assembly factors.^{24,26,27} Our data showing that human ZMYND10 interacts with the reported cytoplasmic dynein assembly factor LRRC6 further supports a role for ZMYND10 in the dynein-arm assembly process that causes PCD when deficient.

Supplemental Data

Supplemental Data include five figures, six tables, and four movies and can be found with this article online at <http://www.cell.com/AJHG>.

Acknowledgments

We would like to thank all the primary ciliary dyskinesia (PCD)-affected families for their participation in the study, Fiona Copeland, and the UK PCD Family Support Group. We wish to acknowledge the contribution of Björn Afzelius, who originally ascertained the GVA-09 family. We thank Jeanette Dankert-Roelse, Maggie Meeks, Celia D. Delozier, and R. Mark Gardiner for family recruitment and their past involvement in the project. We thank Paul Griffin, Sarah Olsson, Mellisa Dixon, Patricia Goggin, Claire Jackson, and Maria Philipsen for light and electron microscopy. We acknowledge technical assistance from Panagiotis Maghsoudlou, Corinne Gehrig, and Anne Vannier. The pBID-UASC-GV plasmid was a gift from B. McCabe. S.E.A. is supported by a Gebert Foundation grant and grants ERC 249968 and SNF 144082. J.-L.B. is supported by grants from the Swiss National Science Foundation (#32003B_135709). J.-L.B., L.B., and H.M.M. are supported by grants from the Milena Carvajal Pro-Kartagener Foundation of Geneva. P.M. is supported by a grant from the Bodossakis Foundation. M.S. is supported by an Action Medical Research UK Clinical Training Fellowship (RTF-1411). A.O., S.P., E.M.K.C., and H.M.M. are supported by Action Medical Research awards GN1773 and GN2101 and Newlife Foundation for Disabled Children UK award 10-11/15. P.I.z.L. and A.P.J. are supported by the Medical Research Council of Great Britain (MR/K018558/10). D.J.M. and G.G. are supported by studentships from the Biotechnology and Biological Sciences Research Council and the Medical Research Council, respectively.

Received: March 28, 2013

Revised: June 21, 2013

Accepted: July 1, 2013

Published: July 25, 2013

Web Resources

The URLs for data presented herein are as follows:

1000 Genomes Project, <http://www.1000genomes.org>

Cilidb, <http://cilidb.cgm.cnrs-gif.fr/>

dbSNP, <http://www.ncbi.nlm.nih.gov/projects/SNP/>

FlyBase, www.flybase.org

NHLBI Exome Variant Server/Sequencing Project (ESP), <http://evs.gs.washington.edu/EVS/>

Online Mendelian Inheritance in Man (OMIM), <http://www.omim.org>

PolyPhen-2, <http://genetics.bwh.harvard.edu/pph2/>

SIFT, <http://sift.jcvi.org/>

References

1. Fliegauf, M., Benzing, T., and Omran, H. (2007). When cilia go bad: cilia defects and ciliopathies. *Nat. Rev. Mol. Cell Biol.* 8, 880–893.
2. Bower, R., Tritschler, D., Vanderwaal, K., Perrone, C.A., Mueller, J., Fox, L., Sale, W.S., and Porter, M.E. (2013). The N-DRC forms a conserved biochemical complex that maintains outer doublet alignment and limits microtubule sliding in motile axonemes. *Mol. Biol. Cell* 24, 1134–1152.
3. Newton, F.G., zur Lage, P.I., Karak, S., Moore, D.J., Göpfert, M.C., and Jarman, A.P. (2012). Forkhead transcription factor Fd3F cooperates with Rfx to regulate a gene expression program for mechanosensory cilia specialization. *Dev. Cell* 22, 1221–1233.
4. Broadhead, R., Dawe, H.R., Farr, H., Griffiths, S., Hart, S.R., Portman, N., Shaw, M.K., Ginger, M.L., Gaskell, S.J., McKean, P.G., and Gull, K. (2006). Flagellar motility is required for the viability of the bloodstream trypanosome. *Nature* 440, 224–227.
5. Lindemann, C.B., and Lesich, K.A. (2010). Flagellar and ciliary beating: the proven and the possible. *J. Cell Sci.* 123, 519–528.
6. Afzelius, B.A. (1998). Genetics and pulmonary medicine. 6. Immotile cilia syndrome: past, present, and prospects for the future. *Thorax* 53, 894–897.
7. Bush, A., Chodhari, R., Collins, N., Copeland, F., Hall, P., Harcourt, J., Hariri, M., Hogg, C., Lucas, J., Mitchison, H.M., et al. (2007). Primary ciliary dyskinesia: current state of the art. *Arch. Dis. Child.* 92, 1136–1140.
8. Barbato, A., Frischer, T., Kuehni, C.E., Snijders, D., Azevedo, I., Baktai, G., Bartoloni, L., Eber, E., Escribano, A., Haarman, E., et al. (2009). Primary ciliary dyskinesia: a consensus statement on diagnostic and treatment approaches in children. *Eur. Respir. J.* 34, 1264–1276.
9. Kennedy, M.P., Omran, H., Leigh, M.W., Dell, S., Morgan, L., Molina, P.L., Robinson, B.V., Minnix, S.L., Olbrich, H., Severin, T., et al. (2007). Congenital heart disease and other heterotaxic defects in a large cohort of patients with primary ciliary dyskinesia. *Circulation* 115, 2814–2821.
10. Bukowy-Bieryłto, Z., Ziętkiewicz, E., Loges, N.T., Wittmer, M., Geremek, M., Olbrich, H., Fliegauf, M., Voelkel, K., Rutkiewicz, E., Rutland, J., et al. (2013). RPGR mutations might cause reduced orientation of respiratory cilia. *Pediatr. Pulmonol.* 48, 352–363.
11. Olbrich, H., Häffner, K., Kispert, A., Völkel, A., Volz, A., Sasmaz, G., Reinhardt, R., Hennig, S., Lehrach, H., Konietzko, N., et al. (2002). Mutations in DNAH5 cause primary ciliary dyskinesia and randomization of left-right asymmetry. *Nat. Genet.* 30, 143–144.

12. Bartoloni, L., Blouin, J.L., Pan, Y., Gehrig, C., Maiti, A.K., Scamuffa, N., Rossier, C., Jorissen, M., Armengot, M., Meeks, M., et al. (2002). Mutations in the DNAH11 (axonemal heavy chain dynein type 11) gene cause one form of situs inversus totalis and most likely primary ciliary dyskinesia. *Proc. Natl. Acad. Sci. USA* 99, 10282–10286.
13. Pennarun, G., Escudier, E., Chapelin, C., Bridoux, A.M., Cacheux, V., Roger, G., Clément, A., Goossens, M., Amselem, S., and Duriez, B. (1999). Loss-of-function mutations in a human gene related to *Chlamydomonas reinhardtii* dynein IC78 result in primary ciliary dyskinesia. *Am. J. Hum. Genet.* 65, 1508–1519.
14. Loges, N.T., Olbrich, H., Fenske, L., Mussaffi, H., Horvath, J., Fliegauf, M., Kuhl, H., Baktai, G., Peterffy, E., Chodhari, R., et al. (2008). DNAI2 mutations cause primary ciliary dyskinesia with defects in the outer dynein arm. *Am. J. Hum. Genet.* 83, 547–558.
15. Mazor, M., Alkhrinawi, S., Chalifa-Caspi, V., Manor, E., Sheffield, V.C., Aviram, M., and Parvari, R. (2011). Primary ciliary dyskinesia caused by homozygous mutation in DNAL1, encoding dynein light chain 1. *Am. J. Hum. Genet.* 88, 599–607.
16. Duriez, B., Duquesnoy, P., Escudier, E., Bridoux, A.M., Escalier, D., Rayet, I., Marcos, E., Vojtek, A.M., Bercher, J.F., and Amselem, S. (2007). A common variant in combination with a nonsense mutation in a member of the thioredoxin family causes primary ciliary dyskinesia. *Proc. Natl. Acad. Sci. USA* 104, 3336–3341.
17. Onoufriadis, A., Paff, T., Antony, D., Shoemark, A., Micha, D., Kuyt, B., Schmidts, M., Petridi, S., Dankert-Roelse, J.E., Haarman, E.G., et al.; UK10K. (2013). Splice-site mutations in the axonemal outer dynein arm docking complex gene CCDC114 cause primary ciliary dyskinesia. *Am. J. Hum. Genet.* 92, 88–98.
18. Knowles, M.R., Leigh, M.W., Ostrowski, L.E., Huang, L., Carson, J.L., Hazucha, M.J., Yin, W., Berg, J.S., Davis, S.D., Dell, S.D., et al.; Genetic Disorders of Mucociliary Clearance Consortium. (2013). Exome sequencing identifies mutations in CCDC114 as a cause of primary ciliary dyskinesia. *Am. J. Hum. Genet.* 92, 99–106.
19. Castleman, V.H., Romio, L., Chodhari, R., Hirst, R.A., de Castro, S.C., Parker, K.A., Ybot-Gonzalez, P., Emes, R.D., Wilson, S.W., Wallis, C., et al. (2009). Mutations in radial spoke head protein genes RSPH9 and RSPH4A cause primary ciliary dyskinesia with central-microtubular-pair abnormalities. *Am. J. Hum. Genet.* 84, 197–209.
20. Olbrich, H., Schmidts, M., Werner, C., Onoufriadis, A., Loges, N.T., Raidt, J., Banki, N.F., Shoemark, A., Burgoyne, T., Al Turki, S., et al.; UK10K Consortium. (2012). Recessive HYDIN mutations cause primary ciliary dyskinesia without randomization of left-right body asymmetry. *Am. J. Hum. Genet.* 91, 672–684.
21. Becker-Heck, A., Zohn, I.E., Okabe, N., Pollock, A., Lenhart, K.B., Sullivan-Brown, J., McSheene, J., Loges, N.T., Olbrich, H., Haeffner, K., et al. (2011). The coiled-coil domain containing protein CCDC40 is essential for motile cilia function and left-right axis formation. *Nat. Genet.* 43, 79–84.
22. Merveille, A.C., Davis, E.E., Becker-Heck, A., Legendre, M., Amirav, I., Bataille, G., Belmont, J., Beydon, N., Billen, F., Clément, A., et al. (2011). CCDC39 is required for assembly of inner dynein arms and the dynein regulatory complex and for normal ciliary motility in humans and dogs. *Nat. Genet.* 43, 72–78.
23. Wirschell, M., Olbrich, H., Werner, C., Tritschler, D., Bower, R., Sale, W.S., Loges, N.T., Pennekamp, P., Lindberg, S., Stenram, U., et al. (2013). The nexin-dynein regulatory complex subunit DRC1 is essential for motile cilia function in algae and humans. *Nat. Genet.* 45, 262–268.
24. Mitchison, H.M., Schmidts, M., Loges, N.T., Freshour, J., Dritsoula, A., Hirst, R.A., O'Callaghan, C., Blau, H., Al Dabbagh, M., Olbrich, H., et al. (2012). Mutations in axonemal dynein assembly factor DNAAF3 cause primary ciliary dyskinesia. *Nat. Genet.* 44, 381–389, S1–S2.
25. Loges, N.T., Olbrich, H., Becker-Heck, A., Häffner, K., Heer, A., Reinhard, C., Schmidts, M., Kispert, A., Zariwala, M.A., Leigh, M.W., et al. (2009). Deletions and point mutations of LRRC50 cause primary ciliary dyskinesia due to dynein arm defects. *Am. J. Hum. Genet.* 85, 883–889.
26. Duquesnoy, P., Escudier, E., Vincensini, L., Freshour, J., Bridoux, A.M., Coste, A., Deschildre, A., de Blic, J., Legendre, M., Montantin, G., et al. (2009). Loss-of-function mutations in the human ortholog of *Chlamydomonas reinhardtii* ODA7 disrupt dynein arm assembly and cause primary ciliary dyskinesia. *Am. J. Hum. Genet.* 85, 890–896.
27. Omran, H., Kobayashi, D., Olbrich, H., Tsukahara, T., Loges, N.T., Hagiwara, H., Zhang, Q., Leblond, G., O'Toole, E., Hara, C., et al. (2008). Ktu/PF13 is required for cytoplasmic pre-assembly of axonemal dyneins. *Nature* 456, 611–616.
28. Panizzi, J.R., Becker-Heck, A., Castleman, V.H., Al-Mutairi, D.A., Liu, Y., Loges, N.T., Pathak, N., Austin-Tse, C., Sheridan, E., Schmidts, M., et al. (2012). CCDC103 mutations cause primary ciliary dyskinesia by disrupting assembly of ciliary dynein arms. *Nat. Genet.* 44, 714–719.
29. Horani, A., Druley, T.E., Zariwala, M.A., Patel, A.C., Levinson, B.T., Van Arendonk, L.G., Thornton, K.C., Giacalone, J.C., Albee, A.J., Wilson, K.S., et al. (2012). Whole-exome capture and sequencing identifies HEATR2 mutation as a cause of primary ciliary dyskinesia. *Am. J. Hum. Genet.* 91, 685–693.
30. Kott, E., Duquesnoy, P., Copin, B., Legendre, M., Dastot-Le Moal, F., Montantin, G., Jeanson, L., Tamalet, A., Papon, J.F., Siffroi, J.P., et al. (2012). Loss-of-function mutations in LRRC6, a gene essential for proper axonemal assembly of inner and outer dynein arms, cause primary ciliary dyskinesia. *Am. J. Hum. Genet.* 91, 958–964.
31. Papon, J.F., Coste, A., Roudot-Thoraval, F., Boucherat, M., Roger, G., Tamalet, A., Vojtek, A.M., Amselem, S., and Escudier, E. (2010). A 20-year experience of electron microscopy in the diagnosis of primary ciliary dyskinesia. *Eur. Respir. J.* 35, 1057–1063.
32. Shoemark, A., Dixon, M., Corrin, B., and Dewar, A. (2012). Twenty-year review of quantitative transmission electron microscopy for the diagnosis of primary ciliary dyskinesia. *J. Clin. Pathol.* 65, 267–271.
33. Chilvers, M.A., Rutman, A., and O'Callaghan, C. (2003). Ciliary beat pattern is associated with specific ultrastructural defects in primary ciliary dyskinesia. *J. Allergy Clin. Immunol.* 112, 518–524.
34. Quinlan, A.R., and Hall, I.M. (2010). BEDTools: a flexible suite of utilities for comparing genomic features. *Bioinformatics* 26, 841–842.
35. Jones, W.D., Dafou, D., McEntagart, M., Woollard, W.J., Elmslie, F.V., Holder-Espinasse, M., Irving, M., Saggart, A.K., Smithson, S., Trembath, R.C., et al. (2012). De novo mutations in MLL cause Wiedemann-Steiner syndrome. *Am. J. Hum. Genet.* 91, 358–364.

36. Abecasis, G.R., Altshuler, D., Auton, A., Brooks, L.D., Durbin, R.M., Gibbs, R.A., Hurler, M.E., and McVean, G.A.; 1000 Genomes Project Consortium. (2010). A map of human genome variation from population-scale sequencing. *Nature* 467, 1061–1073.
37. Arnaiz, O., Malinowska, A., Klotz, C., Sperling, L., Dadlez, M., Koll, F., and Cohen, J. (2009). Cildb: a knowledgebase for centrosomes and cilia. *Database (Oxford)* 2009, bap022.
38. Ross, A.J., Dailey, L.A., Brighton, L.E., and Devlin, R.B. (2007). Transcriptional profiling of mucociliary differentiation in human airway epithelial cells. *Am. J. Respir. Cell Mol. Biol.* 37, 169–185.
39. Geremek, M., Bruinenberg, M., Ziętkiewicz, E., Pogorzelski, A., Witt, M., and Wijmenga, C. (2011). Gene expression studies in cells from primary ciliary dyskinesia patients identify 208 potential ciliary genes. *Hum. Genet.* 129, 283–293.
40. Blouin, J.L., Meeks, M., Radhakrishna, U., Sainsbury, A., Gehring, C., Sail, G.D., Bartoloni, L., Dombi, V., O'Rawe, A., Walne, A., et al. (2000). Primary ciliary dyskinesia: a genome-wide linkage analysis reveals extensive locus heterogeneity. *Eur. J. Hum. Genet.* 8, 109–118.
41. McInerney, E.M., Rose, D.W., Flynn, S.E., Westin, S., Mullen, T.M., Kronen, A., Inostroza, J., Torchia, J., Nolte, R.T., Assamunt, N., et al. (1998). Determinants of coactivator LXXLL motif specificity in nuclear receptor transcriptional activation. *Genes Dev.* 12, 3357–3368.
42. McClintock, T.S., Glasser, C.E., Bose, S.C., and Bergman, D.A. (2008). Tissue expression patterns identify mouse cilia genes. *Physiol. Genomics* 32, 198–206.
43. Agathangelou, A., Dallol, A., Zöschbauer-Müller, S., Morrissey, C., Honorio, S., Hesson, L., Martinsson, T., Fong, K.M., Kuo, M.J., Yuen, P.W., et al. (2003). Epigenetic inactivation of the candidate 3p21.3 suppressor gene BLU in human cancers. *Oncogene* 22, 1580–1588.
44. Chang, J.W., Hsu, H.S., Ni, H.J., Chuang, C.T., Hsiung, C.H., Huang, T.H., and Wang, Y.C. (2010). Distinct epigenetic domains separated by a CTCF bound insulator between the tandem genes, BLU and RASSF1A. *PLoS ONE* 5, e12847.
45. Cachero, S., Simpson, T.I., Zur Lage, P.I., Ma, L., Newton, F.G., Holohan, E.E., Armstrong, J.D., and Jarman, A.P. (2011). The gene regulatory cascade linking proneural specification with differentiation in *Drosophila* sensory neurons. *PLoS Biol.* 9, e1000568.
46. Jarman, A.P. (2002). Studies of mechanosensation using the fly. *Hum. Mol. Genet.* 11, 1215–1218.
47. Liang, X., Madrid, J., Saleh, H.S., and Howard, J. (2011). NOMPC, a member of the TRP channel family, localizes to the tubular body and distal cilium of *Drosophila* campaniform and chordotonal receptor cells. *Cytoskeleton (Hoboken)* 68, 1–7.
48. Göpfert, M.C., Humphris, A.D., Albert, J.T., Robert, D., and Hendrich, O. (2005). Power gain exhibited by motile mechanosensory neurons in *Drosophila* ears. *Proc. Natl. Acad. Sci. USA* 102, 325–330.
49. Göpfert, M.C., and Robert, D. (2003). Motion generation by *Drosophila* mechanosensory neurons. *Proc. Natl. Acad. Sci. USA* 100, 5514–5519.
50. Senthilan, P.R., Piepenbrock, D., Ovezmyradov, G., Nadrowski, B., Bechstedt, S., Pauls, S., Winkler, M., Möbius, W., Howard, J., and Göpfert, M.C. (2012). *Drosophila* auditory organ genes and genetic hearing defects. *Cell* 150, 1042–1054.
51. Marygold, S.J., Leyland, P.C., Seal, R.L., Goodman, J.L., Thurmond, J., Strelets, V.B., and Wilson, R.J.; FlyBase consortium. (2013). FlyBase: improvements to the bibliography. *Nucleic Acids Res.* 41(Database issue), D751–D757.
52. Yu, X., Ng, C.P., Habacher, H., and Roy, S. (2008). Foxj1 transcription factors are master regulators of the motile ciliogenic program. *Nat. Genet.* 40, 1445–1453.
53. Jaquet, B.V., Salinas-Mondragon, R., Liang, H., Therit, B., Buie, J.D., Dykstra, M., Campbell, K., Ostrowski, L.E., Brody, S.L., and Ghashghaei, H.T. (2009). FoxJ1-dependent gene expression is required for differentiation of radial glia into ependymal cells and a subset of astrocytes in the postnatal brain. *Development* 136, 4021–4031.
54. Stubbs, J.L., Oishi, I., Izpisua Belmonte, J.C., and Kintner, C. (2008). The forkhead protein Foxj1 specifies node-like cilia in *Xenopus* and zebrafish embryos. *Nat. Genet.* 40, 1454–1460.
55. Dubruille, R., Laurençon, A., Vandaele, C., Shishido, E., Coulon-Bublex, M., Swoboda, P., Couble, P., Kernan, M., and Durand, B. (2002). *Drosophila* regulatory factor X is necessary for ciliated sensory neuron differentiation. *Development* 129, 5487–5498.
56. Lee, J., Moon, S., Cha, Y., and Chung, Y.D. (2010). *Drosophila* TRPN(=NOMPC) channel localizes to the distal end of mechanosensory cilia. *PLoS ONE* 5, e11012.
57. Fatima, R. (2011). *Drosophila* Dynein intermediate chain gene, Dic61B, is required for spermatogenesis. *PLoS ONE* 6, e27822.
58. Raff, E.C., Hoyle, H.D., Popodi, E.M., and Turner, F.R. (2008). Axoneme beta-tubulin sequence determines attachment of outer dynein arms. *Curr. Biol.* 18, 911–914.
59. Kavlie, R.G., Kernan, M.J., and Eberl, D.F. (2010). Hearing in *Drosophila* requires TilB, a conserved protein associated with ciliary motility. *Genetics* 185, 177–188.
60. Eberl, D.F., Hardy, R.W., and Kernan, M.J. (2000). Genetically similar transduction mechanisms for touch and hearing in *Drosophila*. *J. Neurosci.* 20, 5981–5988.
61. Giot, L., Bader, J.S., Brouwer, C., Chaudhuri, A., Kuang, B., Li, Y., Hao, Y.L., Ooi, C.E., Godwin, B., Vitols, E., et al. (2003). A protein interaction map of *Drosophila melanogaster*. *Science* 302, 1727–1736.
62. Chen, W., and Roeder, R.G. (2011). Mediator-dependent nuclear receptor function. *Semin. Cell Dev. Biol.* 22, 749–758.
63. Rual, J.F., Venkatesan, K., Hao, T., Hirozane-Kishikawa, T., Dricot, A., Li, N., Berriz, G.F., Gibbons, F.D., Dreze, M., Ayivi-Guedehoussou, N., et al. (2005). Towards a proteome-scale map of the human protein-protein interaction network. *Nature* 437, 1173–1178.
64. Hyde, S.J., Eckenroth, B.E., Smith, B.A., Eberley, W.A., Heintz, N.H., Jackman, J.E., and Doublie, S. (2010). tRNA(His) guanylyltransferase (THG1), a unique 3'-5' nucleotidyl transferase, shares unexpected structural homology with canonical 5'-3' DNA polymerases. *Proc. Natl. Acad. Sci. USA* 107, 20305–20310.
65. Kester, H.A., Blanchetot, C., den Hertog, J., van der Saag, P.T., and van der Burg, B. (1999). Transforming growth factor-beta-stimulated clone-22 is a member of a family of leucine zipper proteins that can homo- and heterodimerize and has transcriptional repressor activity. *J. Biol. Chem.* 274, 27439–27447.
66. Brown, M.C., Curtis, M.S., and Turner, C.E. (1998). Paxillin LD motifs may define a new family of protein recognition domains. *Nat. Struct. Biol.* 5, 677–678.